FEN ve MÜHENDİSLİK BİLİMLERİ DERGİSİ

Vol: 7 No: 1 Year: 2025 Araştırma Makalesi/Research Article e-ISSN: 2667-7989

https://doi.org/10.47112/neufmbd.2025.78

H_2O_2'nin SO_3H ile Fonksiyonelleştirilmiş Aktif Karbon/Co-B Nanokompozitleri ile Elektrokimyasal Tespiti

Sümeyye SARIKAYA[1] Görkem TASAR[1] Hasan Hüseyin İPEKCİ[1*] Aytekin UZUNOĞLU[1,2]

[1] Necmettin Erbakan University, Faculty of Engineering, Department of Metallurgical and Material Engineering, Konya, Türkiye

[2] İstanbul Technical University, Faculty of Chemistry- Metallurgical, Department of Metallurgical and Material Engineering, Konya, Türkiye

Makale Bilgisi

Geliş Tarihi: 04.04.2024
Kabul Tarihi: 24.07.2024
Yayın Tarihi: 30.04.2025

Anahtar Kelimeler:
Aktif Karbon,
Elektrokimyasal Sensör,
Hidrojen Peroksit,
Kobalt-bor.

ÖZET

Hidrojen peroksitin farmasötikten klinik ve çevresel uygulamalara ve gıda uygulamalarına kadar çeşitli alanlarda yaygın olarak kullanıldığı göz önüne alındığında, canlı sağlığı üzerindeki zararlı etkileri önemli bir sorundur. Bu nedenle, H_2O_2'nin hızlı, doğru, ucuz ve hassas yöntemlerle tespiti büyük talep görmektedir. Bu çalışmada, oldukça duyarlı H_2O_2 sensörleri oluşturmak için yeni bir katalizör kompozisyonu önerilmiştir. Bu bağlamda, ticari olarak aktifleştirilmiş karbon yüzeyini önce -SO_3H gruplarıyla modifiye edilmiş ve ardından H_2O_2'ye karşı yüksek elektrokatalitik aktivite elde etmek için amorf kobalt-boron fazı kullanılmıştır. Co-B@AC-SO_3H örnekleri SEM, TEM, XPS, XRD ve Raman spektroskopisi kullanılarak karakterize edilmiştir. XRD sonuçlarıyla amorf bir Co-B fazının varlığı doğrulanmış ve XRD ve Raman sonuçlarında karakteristik aktifleştirilmiş karbon tepe noktaları gösterilmiştir. Co-B@AC-SO_3H/GCE tabanlı sensörler, AC/GCE ve AC-SO_3H/GCE tabanlı karşılaştırma yapıldığında çok daha iyi duyarlılık göstermiştir. Sensörler, gerçek örneklerde H_2O_2 tespiti için yüksek depolama stabilitesi ve yüksek güvenilirlik göstermiştir.

Electrochemical Detection of H_2O_2 with SO_3H-functionalized Activated Carbon/Co-B Nanocomposites

Article Info

Received: 04.04.2024
Accepted: 24.07.2024
Published: 30.04.2025

Keywords:
Active Carbon,
Cobalt-Boron,
Electrochemical Sensor,
Hydrogen Peroxide,

ABSTRACT

While hydrogen peroxide has been widely used in various applications ranging from pharmaceutical to clinical and environmental to food applications, its harmful effects on health are an important challenge. Therefore, the detection of H_2O_2 with fast, accurate, cheap, and sensitive methods is in great demand. In this work, we proposed a novel catalyst composition to construct highly sensitive H_2O_2 sensors. In this study, we modified the surface of commercial activated carbon with first -SO_3H groups and then the amorphous cobalt-boron phase to achieve high electrocatalytic activity toward H_2O_2. The Co-B@AC-SO_3H samples were characterized using SEM, TEM, XPS, XRD, and Raman spectroscopy. XRD results confirmed the presence of an amorphous Co-B phase and the characteristic activated carbon peaks were obtained in both XRD and Raman results. The Co-B@AC-SO_3H/GCE-based sensors showed much improved sensitivity compared to AC/GCE and AC-SO_3H/GCE-based counterparts. The sensors showed high storage stability and reliability in detecting H_2O_2 in real samples.

To cite this article:
Sarıkaya, S., Tasar, G., İpekci, H.H. & Uzunoğlu, A. (2025). Electrochemical detection of H_2O_2 with SO_3H-functionalized activated carbon/Co-B nanocomposites. *Necmettin Erbakan University Journal of Science and Engineering, 7*(1), 103-114. https://doi.org/10.47112/neufmbd.2025.78

***Corresponding Author:** Hasan Hüseyin İpekci, *hsnpkc@gmail.com*

INTRODUCTION

The development of electrochemical sensors with high accuracy, good selectivity, wide linear range, and low limit of detection has been a focus of research to enhance the practical applicability of sensors against various analytes including glucose [1], hydrogen peroxide (H_2O_2) [2], dopamine [3], uric acid [4], ascorbic acid [5], and so on. Electrochemical sensors are classified into two main sub-classes: enzymatic and non-enzymatic electrochemical sensors. While enzymatic sensors pose various advantages including high specificity and sensitivity, the denaturation of enzymes depending on the storage conditions is one of the main challenges [6]. In addition, the use of biological enzymes on the electrode surface as the detection layer increases the cost of the electrochemical sensors, which hinders their wide use and practical applications. Therefore, the research focused on the development of novel non-enzymatic electrochemical sensors became a hot topic in electrochemical sensor research. In non-enzymatic sensors, the enzyme layer is replaced by enzyme-mimicking nanomaterials, which in turn enhances the storage stability and lowers the cost of the electrochemical sensors [7]. So far, various carbon-based materials have been implemented in the construction of non-enzymatic electrochemical sensors such as activated carbon [8], carbon nanotubes [9], graphene [10], graphene-related materials, and graphdiyne [11,12]. Among those different carbon allotropes, activated carbon has gained a great focus owing to its low cost, large physical surface area, ease of surface functionalization, high electronic conductivity, and high chemical stability [8]. The reported studies indicated that the modification of carbon surface with nanoparticles is one of the effective ways to achieve high electrochemical activity. This is because carbon itself without defects or nanoparticle decoration shows low electrochemical activity due to its chemical inertness. So far, various noble, non-noble metal and metal oxide nanoparticles have been used to decorate the surface of carbon-based materials to enhance the sensing, mechanical an antifungal performance of the materials [13–15]. On the other hand, especially the use of noble-metal nanoparticles on carbon surfaces increases the cost of sensor fabrication [3].

Hydrogen peroxide has been widely exploited in different applications ranging from pharmaceutical to clinical and environmental to food. Owing to its oxidizing nature, it is also used in disinfectants. While its wide use in various applications, the interaction of H_2O_2 with biological molecules in cells may cause peroxidation of lipids of the cell membrane and proteins, resulting in enzyme denaturation in the cells and damage to DNA. For this reason, the determination of H_2O_2 level with high accuracy, sensitivity, and selectivity in complex media is of great interest to human health. While different conventional analytical tools have been implemented to determine the H_2O_2 level such as chemical titration, fluorescence [16], chemiluminescence [17], spectrophotometry [18], and high-performance liquid chromatography [19]; those methods require a trained person to conduct the experiments, and the experiments are time-consuming and require complex sample preparation steps. Therefore, electrochemical sensors show great promise in detecting H_2O_2 in a cost-effective, fast, and accurate manner.

Among various metal and metal oxide alloy nanoparticles, cobalt-boron-based nanoparticles show improved electrocatalytic performance due to the electron interaction between Co and B atoms by making the Co electroactive sites [20]. While Co-B-based catalysts have been widely used in the hydrolysis of $NaBH_4$ for hydrogen production, their use in electrochemical sensors has not been reported. In the given study, we designed a novel catalyst structure consisting of sulfonate ($-SO_3H$)-functionalized activated carbon-supported Co-B nanoparticles for the detection of H_2O_2. Modifying activated carbon with $-SO_3H$ enables the immobilization of highly dispersed, nanosized metal and metal oxide nanoparticles [1,21,22]. In the given work, we designed a novel catalyst hybrid consisting of cobalt-boron decorated SO_3H-functionalized activated carbon to develop highly sensitive electrochemical H_2O_2 sensors. The catalysts were characterized using X-ray diffraction (XRD), scanning electron microscopy (SEM), transmission electron microscopy (TEM), Raman spectroscopy,

and X-ray photoelectron spectroscopy (XPS). The sensor performance was evaluated using cyclic voltammetry and chronoamperometry methods.

MATERIALS AND METHODS

Sulfonic acid, sodium nitrate, sodium borohydride, cobalt (II) chloride hexahydrate ($CoCl_2.6H_2O$), ethanol, and Nafion® 117 solutions were purchased from Sigma-Aldrich. Active carbon was obtained from Nanografi from Turkey. Sodium hydroxide was purchased from Riedel-de Haën Company.

Preparation of AC-SO_3H Nanoparticles

300 mg of activated carbon (AC) was sonicated in 30 ml DI for 10 minutes using an ultrasonic bath. The suspension was then stirred at 700 rpm in an ice bath using a magnetic stirrer. Sulfonic acid was dissolved in another beaker containing NaOH/DI solution. A certain amount of sodium nitrate was added to the beaker and sonicated for 5 additional minutes in an ultrasonic bath, which was flowed by stirring in an ice bath at 700 rpm using a magnetic stirrer. The obtained mixture was then added to the AC and DI-containing suspension drop by drop. The mixture was stirred for 5 h in an ice bath. The obtained suspension was centrifuged, and the precipitate was washed with DI and ethanol several times, followed by a drying process at 50 ºC.

Preparation of Co NPs@AC-SO_3H

20 mM CoCl2.6H2O and 100 ml DI water were mixed in an ice bath. 100 mg of AC-SO_3H was dispersed in ethanol and then introduced into a Co-containing solution. The resultant solution was stirred at 1300 rpm for 15 h using a magnetic stirrer in an ice bath. Sodium borohydride was added to the mixture drop by drop and left to stir for an additional hour. After this step, the mixture was centrifuged and washed several times with DI and ethanol. The precipitate was dried in a vacuum oven. The synthesized catalysts were named Co-B@AC-SO_3H. The synthesis route is shown schematically in Figure 1.

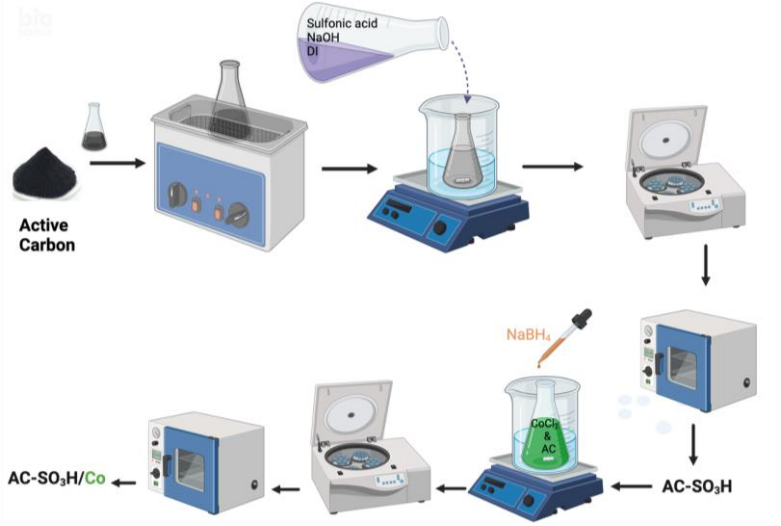

Figure 1
A schematic showing the synthesis route

Characterization of the Catalysts

The phase analysis and bonding properties of the samples were determined using X-ray diffraction and Raman spectroscopy methods. The surface topography and the 2D nanoscale images were obtained using scanning electron (SEM) and transmission electron microscopy (TEM), respectively. The elemental analysis of AC-SO_3H was carried out using X-ray photoelectron spectroscopy (XPS).

Fabrication of Catalysis Ink and Electrochemical Sensors

A glassy carbon electrode (GCE, 3 mm) was first polished with alumina powder and washed with an ethanol/ water mixture in an ultrasonic bath. The catalyst ink was prepared by mixing Co-B@AC-SO_3H, Nafion, ethanol, and DI. 5 µl of the ink was dropped onto a pre-polished GCE surface and dried for 2 h at room temperature. To form a permselective membrane on the sensor surface, a certain amount of Nafion 117 solution (0.05 wt%) was dropped on the sensor surface. The electroanalytical performance of the sensors was evaluated using cyclic voltammetry (CV) and amperometry (CA) methods using an Ivium Compacstat potentiostat. A three-electrode setup was used, in which the glassy carbon electrode (GCE), Ag/AgCl electrode (3 M NaCl, 0.195 V vs RHE), and the platinum wire were used as the working, reference, and counter electrodes, respectively. All the electrochemical measurements were performed at 0.01 M PBS with a pH of 7.4 at room temperature, and DI water was used in all experiments.

RESULTS AND DISCUSSION

Physical Characterization of the Samples

The SEM images recorded at different magnifications are given in Figure 2a-c. As observed, the Co-B@AC-SO_3H powder showed an agglomerated structure. The images at high magnifications showed the presence of homogeneously distributed carbon agglomerates as expected. The TEM images (Figure 2d-f) indicated the presence of regular carbon-shaped particles. It should be noted that no Co-B nanoparticle was observed on the carbon surface, which is attributed to the small particle size. This is because as discussed earlier, in the presence of -SO_3H on the surface of substrates, fine metal nanoparticles can be immobilized on the surface. Therefore, it is essential to conduct additional tools to reveal the presence of Co-B in the catalysts. The XRD and Raman results discussed below also indicated the presence of Co-B alloy nanoparticles on the activated carbon surface. Therefore, the TEM images revealed that the Co-B nanoparticles were too small to be observed in the TEM images.

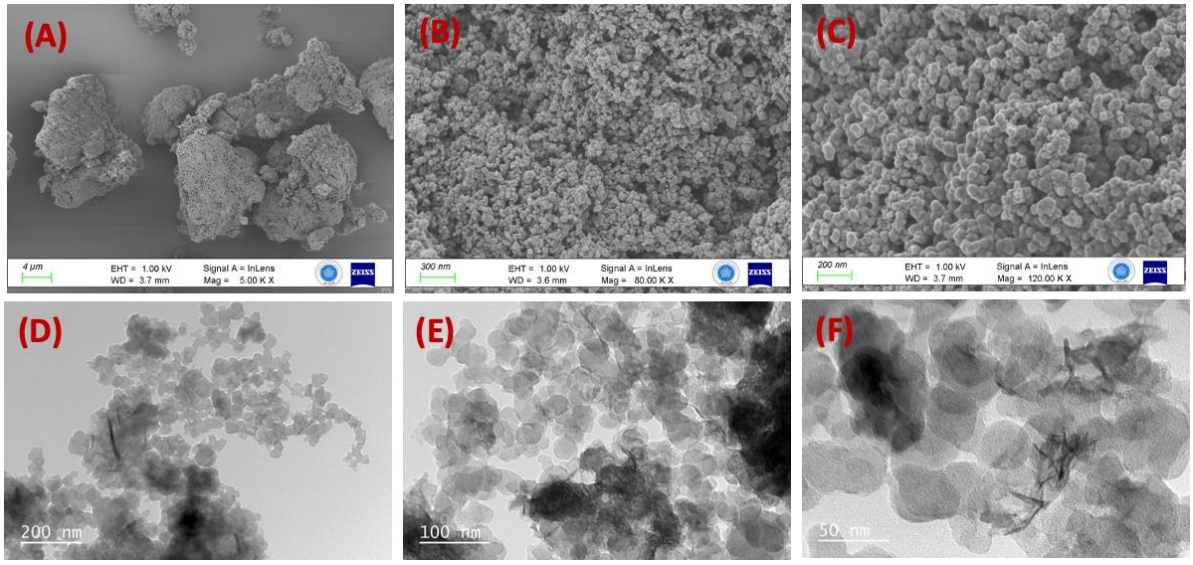

Figure 2
(a-c) SEM and (d-f) TEM images of the samples

The XRD result of Co-B@AC-SO_3H is given in Figure 3a. The characteristic carbon peak was obtained at 25.53°, corresponding to the (002) plane family. In addition, a weak XRD reflection at ca. 43.37° was observed [4]. These results indicated the presence of an amorphous carbon phase. Since Co-B has an amorphous structure, it is not possible to observe the Co-B in the XRD reflection. On the other

hand, XRD reflections with very low intensities located at ca. 44.5° (111) and 51.5° (200) correspond to the crystalline Co nanoparticles (JCPDS #: 15-0806). The presence of diffuse Co reflections indicated the formation of the amorphous Co-B phase in the catalysts. The Raman spectra of the catalyst indicated D and G bands at ca. 1368 and 1603 cm^{-1}, respectively, which are peculiar to the carbon structure. The intensities of the D and G bands (I_D/I_G) were found to be 0.94 and 0.92 for AC-SO_3H and Co-B@AC-SO_3H. Thus, it may be suggested that the decoration of AC-SO_3H with Co-B resulted in a slight recovery in the defect concentration of activated carbon. The Raman reflections observed below 1000 cm^{-1} are ascribed to the Co-containing species.

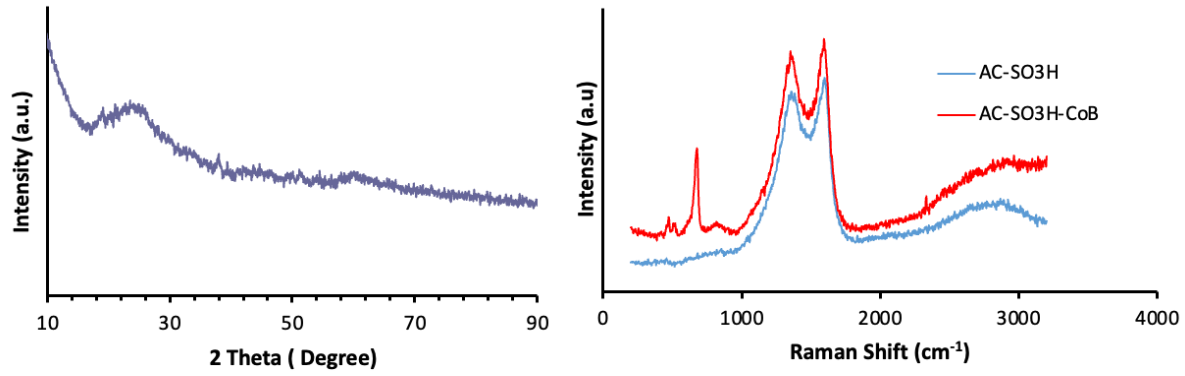

Figure 3
a) XRD and b) Raman Results of the samples

To confirm the -SO_3H modification of activated carbon, AC-SO_3H was analyzed using X-ray photoelectron spectroscopy method. The elemental analysis results indicated that after the sulfonation process, the sample contained S element with 0.25 at.%, indicating the successful modification of the AC surface. The XPS analysis is shown in Figure 4. Figure 4b shows the O1s spectrum with two deconvoluted peaks. The peaks at 532.7 and 534.2 eV correspond to C-O and S=O bonded to organic groups, respectively. The S2p spectrum is deconvoluted into three peaks, S2p 3/2, S2p 1/2, and thiol groups at 168.0 eV, 169.3 eV, and 164.4 eV, respectively (Figure 4c). These results explained that successful sulfonation on the activated carbon surface as SO_3H groups [23,24].

Electrochemical Characterization of the Sensors

The CV behaviors of AC-SO_3H and Co-B@AC-SO_3H-modified GCEs in the absence and presence of H_2O_2 (2 mM) are shown in Figures 5a and b, respectively. While both electrodes did not yield any significant redox peaks in the absence of the analyte, significant reduction peaks were observed with the introduction of H_2O_2, indicating the catalytic activity of the samples. It should be emphasized that the reduction peak current obtained from Co-B@AC-SO_3H was almost twice compared to that obtained from AC-SO_3H, confirming the electrochemical activity of the amorphous Co-B phase in the catalyst layer. The change in the peak current with increasing scan rate is displayed in Figure 5c and the corresponding calibration curve is shown in Figure 5d. As observed, the peak current increased linearly with the square root of the scan rate, indicating that the electrooxidation of H_2O_2 on the sensor surface is a diffusion-controlled reaction [2,25,26].

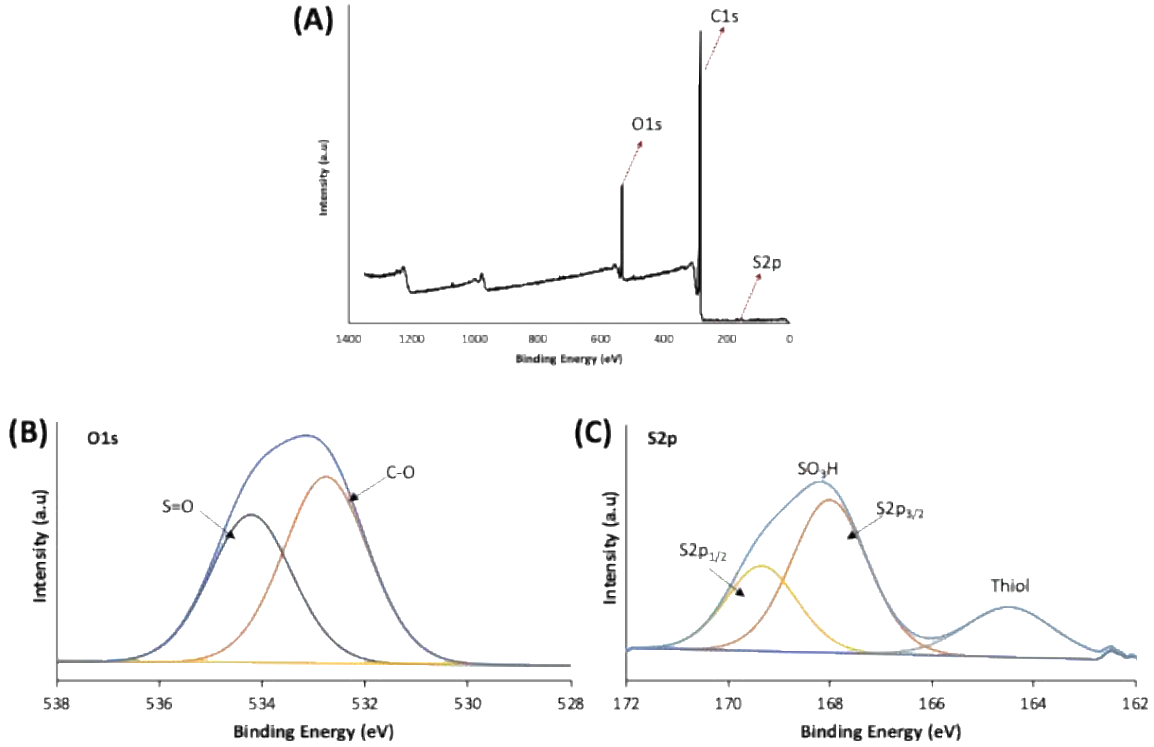

Figure 4

XPS scan a) survey, high resolution for b) O1s, and c) S2p of AC-SO_3H.

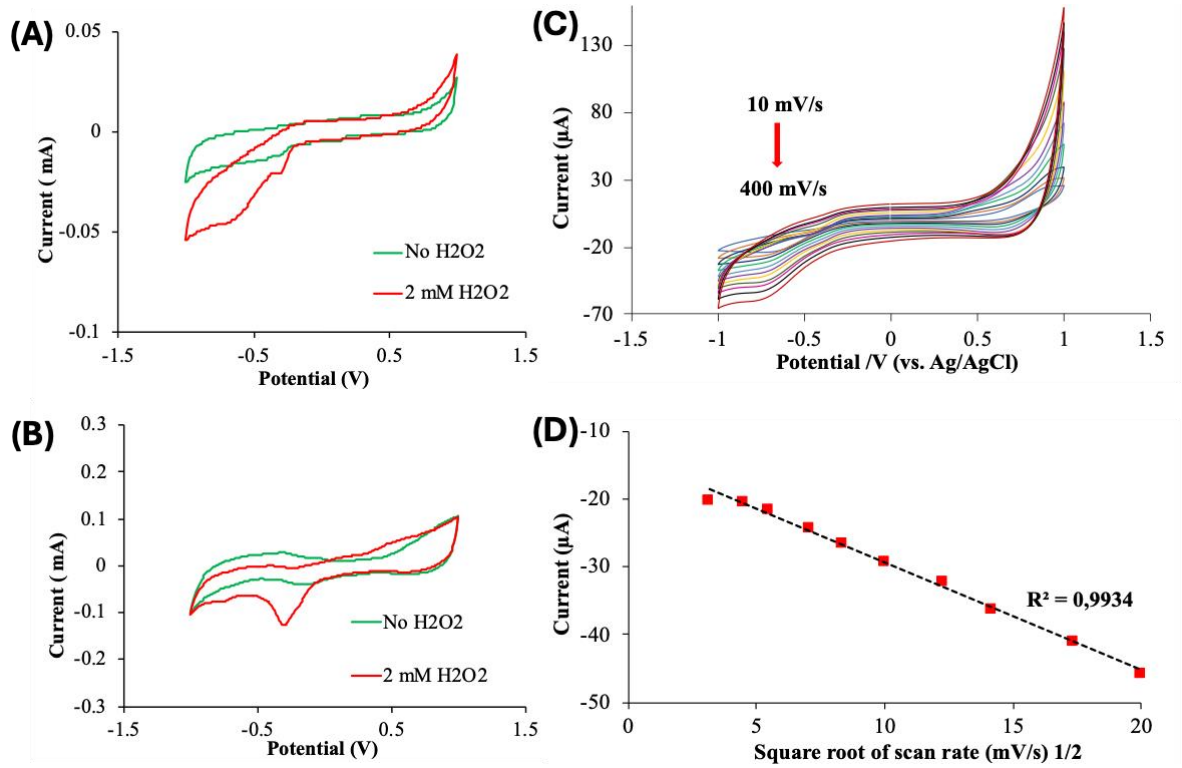

Figure 5

CV curves of a) AC-SO_3H and b) Co-B@AC-SO_3H, c) Effect of scan rate on the peak current of Co-B@AC-SO_3H-based sensors, and d) Corresponding scan rate-peak current graph.

To achieve the highest electrocatalytic performance, the working potential of the sensor was optimized. The calibration (current-concentration) curves obtained from the Co-B@AC-SO_3H/GCE-based sensors at different working potentials are displayed in Figure 6a. The curves showed that the

highest current values were measured at the working potential of 0.6 V. Therefore, further analytical measurements were conducted at that potential. To demonstrate the superior performance of our novel catalyst, we prepared AC/GCE, AC-SO_3H/GCE, and Co-B@AC-SO_3H/GCE-based sensors. The measured current responses toward the successive addition of H_2O_2 are given in Figure 6b. The corresponding calibration curves are displayed in Figure 6c. The highest sensitivity was measured from the Co-B@AC-SO_3H/GCE-based sensors, which is 33.8 and 2.3 times higher than those obtained from AC/GCE and AC-SO_3H/GCE-based sensors, respectively. Therefore, we can allege that the modification of the AC-SO_3H surface with Co-B yielded much higher electrocatalytic activity. The linear ranges of the sensors, however, were almost similar to each other. A high sensitivity of -175.958 ± 7.60 µA $mM^{-1}cm^{-2}$ (RSD%: 4.31, n=3) was achieved from the Co-B@AC-SO_3H/GCE-based sensors. The upper linear range of the sensors was found to be 24 mM. The limit of detection of the Co-B@AC-SO3H/GCE-based sensors was calculated to be 10.8 µM (signal-to-noise ratio of 3). To show the capability of the detection of low H_2O_2 concentrations, H_2O_2 with various concentrations including 10, 30, 50, and 100 µM were introduced and the recorded currents are displayed in Figures 6d and f, which indicate the detection of the analyte with concentrations close to the LOD value. The selectivity of Co-B@AC-SO_3H/GCE-based sensors was studied using glucose (GC), NaCl, ascorbic acid (AA), and uric acid (UA). As displayed in Figure 6e, no significant change in the current response was observed, confirming the high selectivity of the sensors.

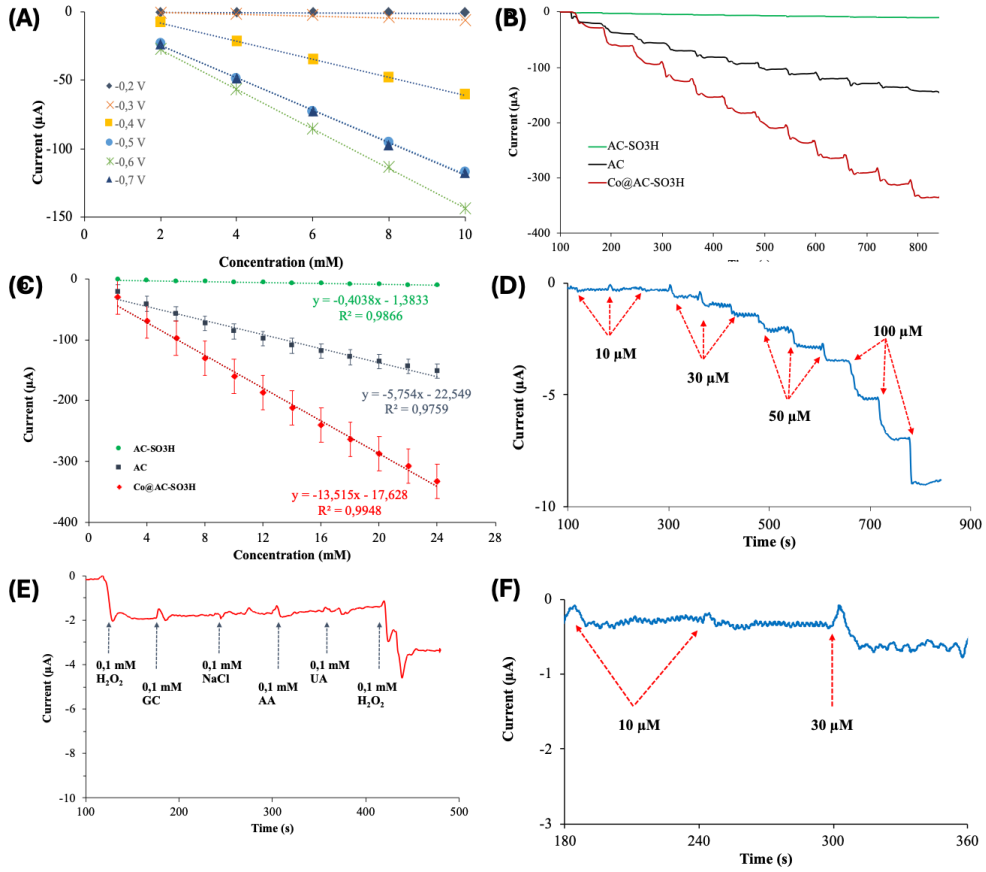

Figure 6

a) Effect of applied voltage on sensor response, b) Chronoamperometry results of AC/GCE, AC- SO_3H/GCE, and Co-B@AC-SO_3H/GCE-based sensors, c) Corresponding calibration curves, d, f) Chronoamperometry results against varying amount of H_2O_2, e) Selectivity of the sensors

The storage stability of the sensors was evaluated by measuring the amperometric response to against 2 mM H_2O_2 for 25 days (n=4). As shown in Figure 7, compared to the initial current (-28.67 ±0.51 µA), after 25 days, the average current response of -29.96 ±0.46 µA was measured. Therefore,

after 25 days, the sensors did not show any drop in current, indicating a high long-term stability. The electrodes were kept at room temperature throughout these experiments.

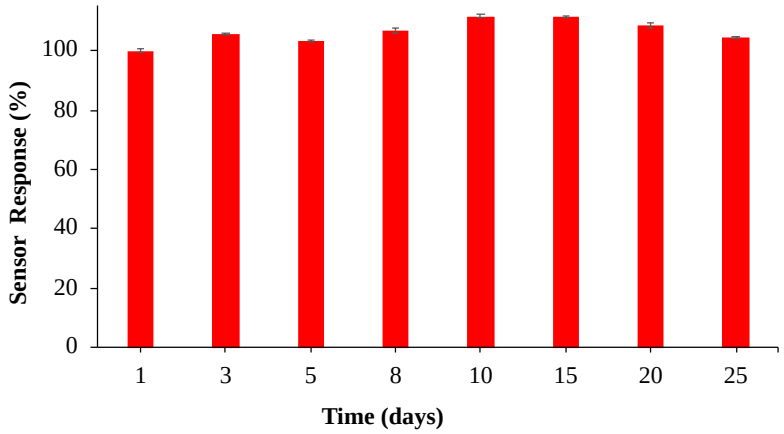

Figure 7
Storage stability of the Co-B@AC-SO_3H/GCE-based sensors (n=4)

Table 1
Comparison of the performance of carbon-based sensors with previously reported sensors

Sensor	Method	Sensitivity ($\mu A\ \mu M^{-1}\ cm^{-2}$)	Linear range (µM)	LOD (µM)	Ref.
rGO/FeNPs/GCE	CA	0.2086	0.1-2150	0.056	[27]
RGO/CNTs-Pt	CA	347 ± 5	0.4-18 10-4x10^3	0.31	[28]
CoHCFNPs/GR/CPE	CA	-	0.6-379.5	0.1	[29]
Co(III)/MWCNT/Nafion	CV	-	0.05-100	0.05	[30]
Vit.B12-NGr	DPV CV	8.775 4.081	2.49-24.5 19.9-167.7	0.02 -	[31]
$CoFe_2O_4$/CNTs/GCE	CA	-	5-50	0.05	[32]
Cu_2O/GNs	CA	-	300-7.8x10^3	20.8	[33]
Au-HS/SO_3H-PMO (Et)	CA	635	0.2-4.3x10^3	0.05	[34]
rGO/CoPc–COOH/GCE	CA	14.5	100–12x10^3	60	[35]
Co-B@AC-SO_3H/GCE	CA	175.958	20-24x10^3	10.8	This work

CoHCFNPs/ GR: Cobalt hexacyanoferrate nanoparticles/graphene, **Vit.B12-NGr:** Vitamin B12 functionalized nitrogen-doped graphene, **$CoFe_2O_4$:** Cobalt ferrite, **Co_3O_4–rGO:** Co_3O_4-reduced graphene oxide, **Cu_2O/GNs:** Cu_2O nanocubes wrapped by graphene nanosheets, **Co_2P/ITO:** Cobalt phosphide/Indium tin oxide, **CoPc–COOH:** Cobalt phthalocyanine tetracarboxylic acid.

Table 2
Detection of H_2O_2 in real samples

Exp. #	Spiked (mM)	Calculated (mM)	Recovery (%)
1	2.0	2.04	102.2
2	4.0	4.07	101.9
3	6.0	6.03	100.5

The performance of the Co-B@AC-SO3H/GCE-based sensors was compared with those reported previously. Some of the recent reports are listed in Table 1. As observed, our novel sensor surface yielded higher performance in terms of linear range and sensitivity. On the other hand, the LOD of our sensor design was higher than those listed in Table 1, suggesting that the LOD of Co-B@AC-SO_3H/GCE-based sensors should be decreased further. The real applicability and the reliability of the sensor response were evaluated by measuring the H_2O_2 concentration in real samples. In this experiment, we evaluated the current response of H_2O_2 in a 3 wt% H_2O_2-containing disinfectant using our sensors. The analytical results were calculated using the measured and calculated H_2O_2 concentrations. Recovery

% values were calculated using calculated and spiked H_2O_2 concentrations based on the equation of Recovery=((calculated/spiked)*100). The calculated value is used to determine the analyte concentration in the spiked sample using the electrochemical method, while spiked refers to the amount of a known analyte concentration containing H_2O_2. As shown in Table 2, the average recoveries are between 100.5% and 102.2%, which indicates that the sensors are effective for the detection of H_2O_2 in practical analysis.

CONCLUSIONS

Herein, we developed a novel catalyst by exploiting the high electrocatalytic activity of the amorphous Co-B phase precipitated on SO_3H-modified activated carbon. The Co-B@AC-SO_3H samples were characterized using SEM, TEM, XPS, XRD, and Raman spectroscopy. The presence of an amorphous Co-B phase was confirmed by XRD results, and the characteristic activated carbon peaks were obtained in both XRD and Raman results. The Co-B@AC-SO_3H/GCE-based sensors showed much improved sensitivity compared with their AC/GCE and AC-SO_3H/GCE-based counterparts. The sensors showed high storage stability and high reliability in detecting H_2O_2 in real samples. Electrochemical sensors have been proven to detect hydrogen peroxide with electrochemical sensors in environmental monitoring applications in a wide range of fields such as food safety, pharmaceuticals, and water treatment. Their high sensitivity, specificity, and real-time analysis capabilities make them ideal for applications requiring accurate and rapid detection. As technology advances, the development of more sophisticated and robust electrochemical sensors will further enhance their use and expand their applications, contributing to safety and quality improvement in many industries.

Ethical Statement

This study is derived from a undergratude thesis entitled ‘Preparation of Active Carbon Based Sensor for Hydrogen Peroxide Determination’ submitted under the supervision of Aytekin Uzunoglu on July 2020.

Author Contributions

Research Design (CRediT 1) H.H.İ. (50%) - A.U. (50%)
Data Collection (CRediT 2) S.S. (50%) - G.T. (50%)
Research - Data Analysis - Validation (CRediT 3-4-6-11) S.S. (30%) - G.T. (20%)-H.H.İ. (%50)
Writing the Article (CRediT 12-13) H.H.İ. (70%) - A.U. (30%)
Revision and Improvement of the Text (CRediT 14) H.H.İ. (70%) - A.U. (30%)

Financing

This study was supported by the Necmettin Erbakan University, Scientific Research Projects Coordination Unit institution with project number 191219009.

Conflict of Interest

The authors declare no conflict of interest.

REFERENCES

[1] M. Dilsen, H.H. Ipekci, A. Uzunoglu, Inkjet printing of Pd/SO3H-modified graphene on different polymeric substrates to construct flexible electrochemical sensors, *Journal of Materials Research*. 38 (2023), 3572-3584. doi:10.1557/S43578-023-01086-7/METRICS

[2] A. Uzunoglu, H.H. Ipekci, The use of CeO2-modified Pt/C catalyst inks for the construction of high-performance enzyme-free H2O2 sensors, *Journal of Electroanalytical Chemistry*. 848 (2019), 113302. doi:10.1016/J.JELECHEM.2019.113302

[3] H.H. Ipekci, Electrochemical Dopamine Detection Using Palladium/Carbon Nano Onion Hybrids, *Hittite Journal of Science and Engineering*. 10 (2023), 201-209. doi:10.17350/HJSE19030000308

[4] H.H. Ipekci, Holey MoS2-based electrochemical sensors for simultaneous dopamine and uric acid detection, *Analytical Methods*. 15 (2023), 2989-2996. doi:10.1039/D3AY00573A

[5] P. Deng, J. Feng, J. Xiao, Y. Wei, X. Liu, J. Li, Q. He, Application of a simple and sensitive electrochemical sensor in simultaneous determination of paracetamol and ascorbic acid, *Journal of The Electrochemical Society*. 168 (2021,) 096501. doi:10.1149/1945-7111/ac1e59

[6] J. Baranwal, B. Barse, G. Gatto, G. Broncova, A. Kumar, Electrochemical sensors and their applications: A review, *Chemosensors*. 10 (2022). doi:10.3390/chemosensors10090363

[7] C. Revathi, R.T. Rajendra kumar, Chapter 7 - Enzymatic and Nonenzymatic Electrochemical Biosensors, içinde: M. Hywel, C.S. Rout, D.J.B.T.-F. and S.A. of 2D M. Late (Ed.), *Woodhead Publishing Series in Electronic and Optical Materials*, *Woodhead Publishing*, 2019: ss. 259-300. doi:10.1016/B978-0-08-102577-2.00007-5

[8] J. Wang, H. Kong, J. Zhang, Y. Hao, Z. Shao, F. Ciucci, Carbon-based electrocatalysts for sustainable energy applications, *Progress in Materials Science*. 116 (2021), 100717. doi:10.1016/j.pmatsci.2020.100717

[9] C.B. Jacobs, M.J. Peairs, B.J. Venton, Review: Carbon nanotube based electrochemical sensors for biomolecules, *Analytica Chimica Acta*. 662 (2010), 105-127. doi:10.1016/j.aca.2010.01.009

[10] Y. Wang, Y. Shao, D.W. Matson, J. Li, Y. Lin, Nitrogen-doped graphene and its application in electrochemical biosensing, *ACS Nano*. 4 (2010), 1790-1798. doi:10.1021/nn100315s

[11] X. Sun, M. Duan, R. Li, Y. Meng, Q. Bai, L. Wang, M. Liu, Z. Yang, Z. Zhu, N. Sui, Ultrathin graphdiyne/graphene heterostructure as a robust electrochemical sensing platform, *Analytical Chemistry*. 94 (2022), 13598-13606. doi:10.1021/acs.analchem.2c03387

[12] E. Ceylan, O. Ozoglu, H.H. Ipekci, A. Tor, A. Uzunoglu, Non-enzymatic detection of methyl parathion in water using CeO2-CuO-decorated reduced graphene oxide, *Microchemical Journal.* 199 (2024), 110261. doi: 10.1016/j.microc.2024.110261

[13] S. Bulbul, E. Ayhan, H. Gökmeşe, Effect on mechanical properties of addition of coal ash as thermal power plant waste to SBR Matrix Compounds, *Necmettin Erbakan University Journal of Science and Engineering*. 5 (2023), 135-146. doi:10.47112/neufmbd.2023.14

[14] İ. Akın, E. Zor, H. Bingöl, Preparation and characterization of GO/Fe3O4 doped polymeric composite membranes, *Necmettin Erbakan University Journal of Science and Engineering*. 5 (2023), 38-52. doi:10.47112/neufmbd.2023.8

[15] K. Çetin, K. Şarkaya, B. Kavakcıoğlu Yardımcı, Antifungal activities of copper (II) ion and histidine incorporated polymers on yeast *Saccharomyces cerevisiae*, *Necmettin Erbakan University Journal of Science and Engineering*. 5 (2023), 267-277. doi:10.47112/neufmbd.2023.24

[16] Y. Zuo, Y. Jiao, C. Ma, C. Duan, A novel fluorescent probe for hydrogen peroxide and its application in bio-imaging, *Molecules*. 26 (2021). doi:10.3390/MOLECULES26113352

[17] W.J. Cooper, J.K. Moegling, R.J. Kieber, J.J. Kiddle, A chemiluminescence method for the analysis of H2O2 in natural waters, *Marine Chemistry*. 70 (2000), 191-200. doi:10.1016/S0304-4203(00)00025-6

[18] K. Sunil, B. Narayana, Spectrophotometric determination of hydrogen peroxide in water and cream samples, *Bulletin of Environmental Contamination and Toxicology*. 81 (2008), 422-426. doi:10.1007/S00128-008-9477-7

[19] P. Gimeno, C. Bousquet, N. Lassu, A.-F. Maggio, C. Civade, C. Brenier, L. Lempereur, High-performance liquid chromatography method for the determination of hydrogen peroxide present or released in teeth bleaching kits and hair cosmetic products, *Journal of Pharmaceutical and Biomedical Analysis*. 107 (2015), 386-393. doi:10.1016/j.jpba.2015.01.018

[20] B. Long, J. Chen, S.W. Sharshir, L. Ibrahim, W. Zhou, C. Wang, L. Wang, Z. Yuan, The mechanism and challenges of cobalt-boron-based catalysts in the hydrolysis of sodium borohydride, *Journal of Materials Chemistry A*. 12 (2024), 5606-5625. doi:10.1039/D3TA07308D

[21] L. Xin, F. Yang, Y. Qiu, A. Uzunoglu, T. Rockward, R.L. Borup, L.A. Stanciu, W. Li, J. Xie, Polybenzimidazole (PBI) functionalized nanographene as highly stable catalyst support for polymer electrolyte membrane fuel cells (PEMFCs), *Journal of The Electrochemical Society*. 163 (2016), F1228-F1236. doi:10.1149/2.0921610JES/XML

[22] L. Xin, F. Yang, S. Rasouli, Y. Qiu, Z.F. Li, A. Uzunoglu, C.J. Sun, Y. Liu, P. Ferreira, W. Li, Y. Ren, L.A. Stanciu, J. Xie, Understanding Pt nanoparticle anchoring on graphene supports through surface functionalization, *ACS Catalysis*. 6 (2016), 2642-2653. doi:10.1021/ACSCATAL.5B02722/ASSET/IMAGES/MEDIUM/CS-2015-02722X_0010.GIF

[23] U.I. Nda-Umar, I. Ramli, E.N. Muhamad, N. Azri, Y.H. Taufiq-Yap, Optimization and characterization of mesoporous sulfonated carbon catalyst and its application in modeling and optimization of acetin production, *Molecules.* 25 (2020), 5221. doi:10.3390/molecules25225221

[24] C.B. Rodella, D.H. Barrett, S.F. Moya, S.J.A. Figueroa, M.T.B. Pimenta, A.A.S. Curvelo, V.T. Silva, Pyhsical and chemical studies of tungsten carbide catalysts: effects of Ni promotion and sulphonated carbon, *RSC Advances.* 5 (2015), 23874. doi:10.1039/c5ra03252k

[25] A. Uzunoglu, S. Song, L.A. Stanciu, A sensitive electrochemical H2O2 sensor based on PdAg-decorated reduced graphene oxide nanocomposites , *Journal of The Electrochemical Society*. 163 (2016), B379-B384. doi:10.1149/2.1201607JES/XML

[26] A. Uzunoglu, A.D. Scherbarth, L.A. Stanciu, Bimetallic PdCu/SPCE non-enzymatic hydrogen peroxide sensors, *Sensors and Actuators B: Chemical*. 220 (2015), 968-976. doi:10.1016/J.SNB.2015.06.033

[27] B. Amanulla, S. Palanisamy, S.M. Chen, V. Velusamy, T.W. Chiu, T.W. Chen, S.K. Ramaraj, A non-enzymatic amperometric hydrogen peroxide sensor based on iron nanoparticles decorated reduced graphene oxide nanocomposite, *Journal of Colloid and Interface Science*. 487 (2017), 370-377. doi:10.1016/J.JCIS.2016.10.050

[28] Y. Zhang, Q. Cao, F. Zhu, H. Xu, Y. Zhang, W. Xu, X. Liao, An amperometric hydrogen peroxide sensor based on reduced graphene oxide/carbon nanotubes/Pt NPs modified glassy carbon electrode, *International Journal of Electrochemical Science*. 15 (2020), 8771-8785. doi:10.20964/2020.09.62

[29] S. Yang, G. Li, G. Wang, J. Zhao, M. Hu, L. Qu, A novel nonenzymatic H2O2 sensor based on cobalt hexacyanoferrate nanoparticles and graphene composite modified electrode, *Sensors and Actuators B: Chemical*. 208 (2015), 593-599. doi:10.1016/J.SNB.2014.11.055

[30] C.M. Parnell, F. Watanabe, U.B. Nasini, B.C. Berry, T. Mitchell, A.U. Shaikh, A. Ghosh, Electrochemical sensing of hydrogen peroxide using a cobalt(III) complex supported on carbonaceous nanomaterials, *Journal of Electroanalytical Chemistry*. 740 (2015), 37-44. doi:10.1016/J.JELECHEM.2014.12.022

[31] S.A. Bhat, N. Rashid, M.A. Rather, S.A. Pandit, P.P. Ingole, M.A. Bhat, Vitamin B12 functionalized N-Doped graphene: A promising electro-catalyst for hydrogen evolution and electro-oxidative sensing of H2O2, *Electrochimica Acta*. 337 (2020), 135730. doi:10.1016/J.ELECTACTA.2020.135730

[32] S. Sahoo, P.K. Sahoo, S. Manna, A.K. Satpati, A novel low cost nonenzymatic hydrogen peroxide sensor based on CoFe2O4/CNTs nanocomposite modified electrode, *Journal of Electroanalytical Chemistry*. 876 (2020), 114504. doi:10.1016/J.JELECHEM.2020.114504

[33] M. Liu, R. Liu, W. Chen, Graphene wrapped Cu2O nanocubes: Non-enzymatic electrochemical sensors for the detection of glucose and hydrogen peroxide with enhanced stability, *Biosensors and Bioelectronics*. 45 (2013), 206-212. doi:10.1016/J.BIOS.2013.02.010

[34] F. Jia, H. Zhong, F. Zhu, X. Li, Y. Wang, Z. Cheng, L. Zhang, Z. Sheng, L. Guo, Nonenzymatic hydrogen peroxide electrochemical sensor based on Au-HS/SO3H-PMO (Et) nanocomposite, *Electroanalysis*. 26 (2014), 2244-2251. doi:10.1002/ELAN.201400318

[35] I.S. Hosu, Q. Wang, A. Vasilescu, S.F. Peteu, V. Raditoiu, S. Railian, V. Zaitsev, K. Turcheniuk, Q. Wang, M. Li, R. Boukherroub, S. Szunerits, Cobalt phthalocyanine tetracarboxylic acid modified reduced graphene oxide: a sensitive matrix for the electrocatalytic detection of peroxynitrite and hydrogen peroxide, *RSC Advances*. 5 (2014), 1474-1484. doi:10.1039/C4RA09781E